Neuron
Article

Pyramidal Neurons Derived from Human Pluripotent Stem Cells Integrate Efficiently into Mouse Brain Circuits In Vivo

Ira Espuny-Camacho,[1] Kimmo A. Michelsen,[1] David Gall,[2] Daniele Linaro,[5] Anja Hasche,[1] Jérôme Bonnefont,[1] Camilia Bali,[1] David Orduz,[2] Angéline Bilheu,[1] Adèle Herpoel,[1] Nelle Lambert,[1,8] Nicolas Gaspard,[1] Sophie Péron,[4] Serge N. Schiffmann,[2] Michele Giugliano,[5,6,7] Afsaneh Gaillard,[4,*] and Pierre Vanderhaeghen[1,3,*]

[1]Université Libre de Bruxelles (U.L.B.), Institut de Recherches en Biologie Humaine et Moléculaire (IRIBHM), and ULB Neuroscience Institute (UNI), B-1070 Brussels, Belgium
[2]Laboratory of Neurophysiology and ULB Neuroscience Institute (UNI)
[3]Welbio
Université Libre de Bruxelles (U.L.B.), B-1070 Brussels Belgium
[4]INSERM U-1084, Experimental and Clinical Neurosciences Laboratory, Cellular Therapies in Brain Diseases group, University of Poitiers, F-86022 Poitiers, France
[5]Theoretical Neurobiology and Neuroengineering Laboratory, Department of Biomedical Sciences, University of Antwerp, B-2610 Wilrijk, Belgium
[6]Laboratory of Neural Microcircuitry, Brain Mind Institute, Swiss Federal Institute of Technology (EPFL), CH-1015 Lausanne, Switzerland
[7]Department of Computer Science, University of Sheffield, Sheffield S102TN, UK
[8]Medical Genetics Department, Université Libre de Bruxelles, Hôpital Erasme, B-1070 Brussels, Belgium
*Correspondence: afsaneh.gaillard@univ-poitiers.fr (A.G.), pierre.vanderhaeghen@ulb.ac.be (P.V.)
http://dx.doi.org/10.1016/j.neuron.2012.12.011

SUMMARY

The study of human cortical development has major implications for brain evolution and diseases but has remained elusive due to paucity of experimental models. Here we found that human embryonic stem cells (ESCs) and induced pluripotent stem cells (iPSCs), cultured without added morphogens, recapitulate corticogenesis leading to the sequential generation of functional pyramidal neurons of all six layer identities. After transplantation into mouse neonatal brain, human ESC-derived cortical neurons integrated robustly and established specific axonal projections and dendritic patterns corresponding to native cortical neurons. The differentiation and connectivity of the transplanted human cortical neurons complexified progressively over several months in vivo, culminating in the establishment of functional synapses with the host circuitry. Our data demonstrate that human cortical neurons generated in vitro from ESC/iPSC can develop complex hodological properties characteristic of the cerebral cortex in vivo, thereby offering unprecedented opportunities for the modeling of human cortex diseases and brain repair.

INTRODUCTION

The cerebral cortex is a complex cellular mosaic containing dozens of neuronal subtypes that display specific connectivity with the rest of the brain and thereby subserve highly diverse and elaborate functions.

Pyramidal neurons constitute more than 80% of cortical neurons and are further diversified in distinct cortical layers to establish specific patterns of axonal output and dendritic input, providing the essential substrate of cortical circuitry (Hevner, 2006; Molnár and Cheung, 2006; Molyneaux et al., 2007). For instance, layer VI neurons send their main projections to the thalamus, while most projections to midbrain, hindbrain, and spinal cord emerge from layer V neurons. Neurons from layer II/III, together with a subset of neurons from layer V, contribute to most intracortical projections, including the callosal projections to the contralateral cerebral hemisphere. In parallel, the cortical surface is parcellated into functional areas displaying modality-specific patterns of connectivity with the rest of the brain, such that, for instance, motor cortex will connect preferentially with thalamic and hindbrain motor nuclei and spinal cord, whereas visual cortex will project to visual centers in thalamus and midbrain (O'Leary and Sahara, 2008; Sur and Rubenstein, 2005; Vanderhaeghen and Polleux, 2004).

The cortex has undergone considerable complexification during recent primate evolution, characterized by an increase in the number and diversity of cortical neurons, additional cortical areas, and a relative expansion of cortical thickness (Hill and Walsh, 2005; Lui et al., 2011; Rakic, 2009). This evolution is probably linked to differences in the developmental features of corticogenesis (Bystron et al., 2008; Fish et al., 2008; Lui et al., 2011). These include longer phases of expansion of early cortical progenitors and prolonged periods of neurogenesis, taking several months in the human to allow the generation of many more cortical neurons (Bystron et al., 2006; Caviness et al., 1995; Rakic, 2009). In addition, late aspects of cortical neuronal differentiation, such as dendritic and synaptic maturation, are also protracted in time, and this neoteny may confer higher postnatal plasticity to the developing human brain (Defelipe, 2011; Petanjek et al., 2011).

Despite recent progress (Lui et al., 2011), the study of human-specific aspects of brain development has remained difficult. The advent of pluripotent stem cells, including embryonic stem cells (ESCs) and induced pluripotent stem cells (iPSCs) offers new opportunities to model human neural development and diseases (Dolmetsch and Geschwind, 2011; Han et al., 2011; Marchetto et al., 2010; Zhang et al., 2010). Directed differentiation of cortical neurons was previously described from mouse ESC (Eiraku et al., 2008; Gaspard et al., 2008). We reported the directed differentiation of mouse ESC into cortical neurons cultured without any morphogen (Gaspard et al., 2008, 2009), thus recapitulating the in vivo primitive pathway of forebrain induction (Wilson and Houart, 2004). After grafting in neonatal mouse brain, mouse ESC-derived cortical pyramidal neurons sent projections similar to those of the host cortex, providing demonstration of their cortical identity (Gaspard et al., 2008).

Although the generation of pyramidal neurons was also reported from human ESC/iPSC (Eiraku et al., 2008; Li et al., 2009; Shi et al., 2012; Zeng et al., 2010), it has remained unclear whether the mouse intrinsic pathway, followed in the absence of exogenous morphogens, was conserved in human cells. Besides, and most importantly, the exact identity of the human ESC-derived neurons generated has remained uncertain, since cardinal hodological features of cortical neurons, such as their patterns of axonal and dendritic projections, have never been tested by in vivo grafting.

Here, we show that the major hallmarks of corticogenesis can be recapitulated from human ESC and iPSC in the absence of added morphogens, up to the sequential generation of functional pyramidal neurons of diverse layer identities. After grafting in the mouse neonatal brain, human ESC-derived cortical neurons displayed robust and specific patterns of axonal projections and dendritic outgrowth and integrated functionally with the host synaptic circuitry, after a human-specific timeline. This enables the study of human cortex development and diseases in an in vivo context.

RESULTS

An Intrinsic Pathway from Human ESC/iPSC to Cortical Pyramidal Neurons

To determine whether the mouse ESC intrinsic pathway of corticogenesis (Gaspard et al., 2008) was conserved in human ESC, we adapted default culture conditions (Gaspard et al., 2009) to allow human cells to survive without added morphogens (see Experimental Procedures for details), supplemented with bone morphogenic protein (BMP) inhibitor Noggin to increase the rate of neural induction from human ESC and iPSC (Chambers et al., 2009; Pera et al., 2004). Over 10–19 days in vitro (DIV), human ESC mostly differentiated into Nestin-positive neural progenitors that coexpressed Pax6 and Otx1/2, consistent with the identity of early dorsal forebrain primordium (Inoue et al., 2000; Walther and Gruss, 1991) (Figures 1A and 1B and see Figure S2B available online). Quantitative RT-PCR (qRT-PCR) analyses revealed the gradual appearance of markers of neural progenitor (*SOX1/BLBP*) and of cortical identity (*OtX1/EMX1/EMX2/FOXG1/PAX6/TBR2/TBR1*) (Figures 1C and 1D, Figure S2A). This pattern of regional identity was further investigated by microarray gene profiling experiments, in which the transcriptome of early differentiating cortical-like cells (24 DIV) was compared with those of undifferentiated human ESC and of human embryonic dorsal telencephalon at 9 gestational weeks (GWs). This revealed a strong upregulation of genes corresponding to telencephalon and/or cortical identity (Hébert and Fishell, 2008) during ESC-cortical differentiation, in striking similarity with the pattern of expression of the fetal cortical samples (Figure S2H). Conversely, the expression of markers of more caudal neural regions remained low in the hESC-derived neural cells as well as in the cortical human samples.

Notably, this robust telencephalic and/or cortical induction was only obtained after long (16 day) treatments with Noggin in vitro, as shorter treatments resulted in induction of genes corresponding mostly to diencephalon (*IRX3/GBX2*) (Figures 1C and 1D). Similar patterns of forebrain and/or cortical induction were obtained from different lines of ESC and iPSC (generated in this study; Figures S1 and S2C–S2G). Interestingly, unlike in mouse ESC corticogenesis (Gaspard et al., 2008), the induction of cortical identity did not require the inhibition of the Sonic Hedgehog (SHH) pathway, as previously reported (Li et al., 2009). Indeed, while SHH treatments resulted in expected ventral forebrain fates, cyclopamine (an inhibitor of SHH) did not result in significant changes in progenitor identity (Figure S3). These data show that in the absence of added morphogens but in the prolonged presence of the BMP inhibitor Noggin, human pluripotent stem cells efficiently convert to a population of neural progenitors that mostly correspond to a cortical identity.

We next assessed the identity, maturation, and functionality of the neurons generated from these progenitors. The majority of the βIII-tubulin-positive neurons expressed the vesicular glutamate transporters 1/2 (VGLUT1/2) (Figures 1E and 1H) and displayed a unipolar and pyramidal morphology index (PMI) (Hand et al., 2005) corresponding to cortical glutamatergic pyramidal neurons (Figures 1F and 1G). After more than 2 months in culture, the neurons expressed markers of functionality, such as the presynaptic marker synaptophysin and the postsynaptic marker HOMER 1 (Figures 1I and 1J). Neuronal maturation during the human ESC-differentiation was further assessed by microarray profiling, in which the transcriptomes of ESC-derived differentiating cortical-like cells were compared with those of undifferentiated ESC and samples of human embryonic dorsal telencephalon at 9 GW and dissected cortical plate (thus containing mostly neurons) at 19 GW (Figure 1K). This revealed a gradual upregulation of genes typically expressed in mature neurons (http://cbl-gorilla.cs.technion.ac.il), culminating after 61–72 DIV, according to a pattern that is intermediate between those observed for human fetal cortical samples at 9 and 19 GW (Figure 1K; Tables S2 and S3).

We next determined more directly the functionality of the neurons, first by calcium imaging, which demonstrated spontaneous calcium waves that were blocked by tetrodotoxin (TTX) (Figure S4A and Movie S1). To confirm and characterize the functional maturation of ESC-derived neurons with time, we performed patch-clamp recordings, focusing on the evolution of passive membrane properties, excitability, and synaptic currents. This revealed a temporal evolution in the

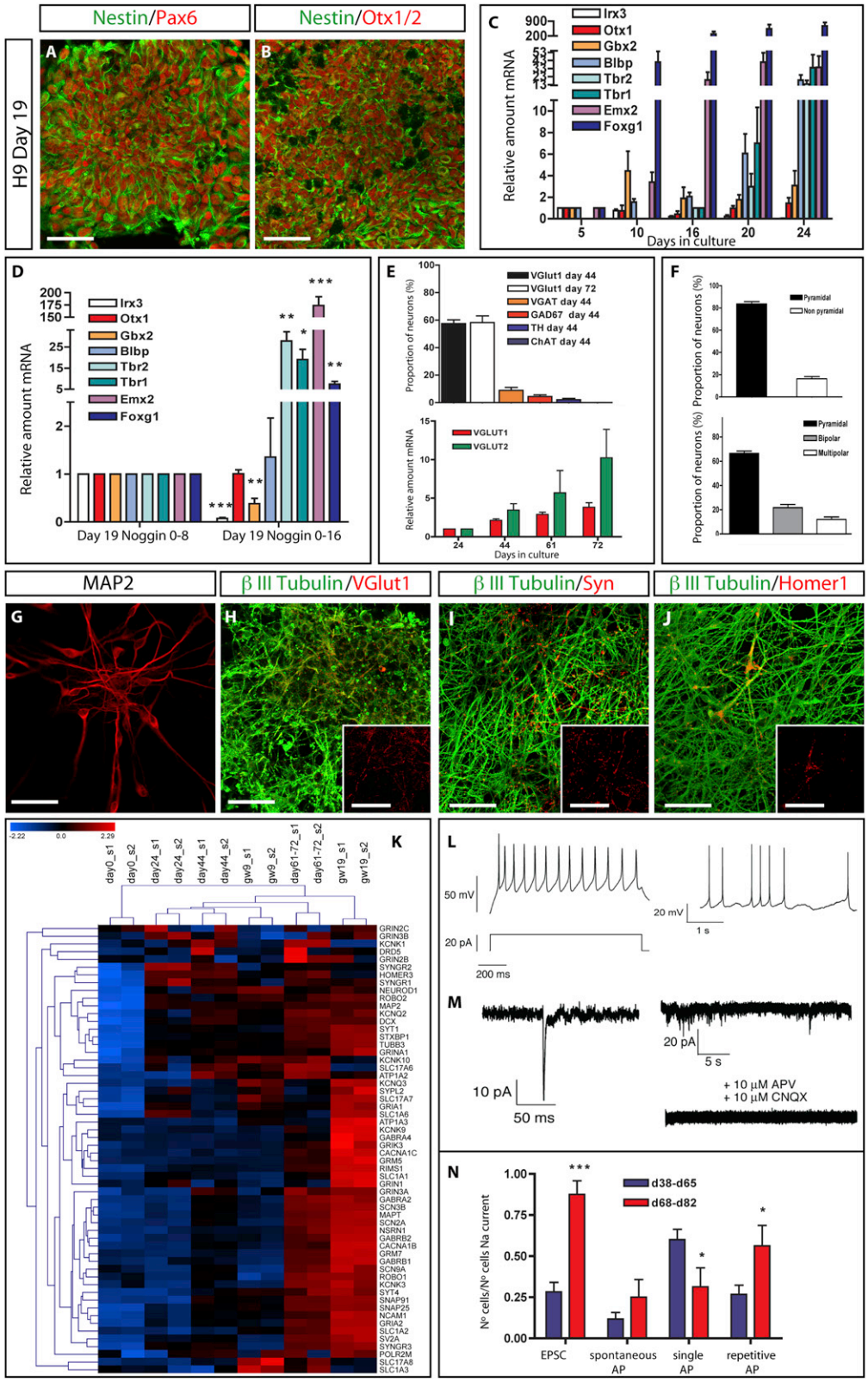

Figure 1. Default Generation of Functional Cortical Pyramidal Neurons from Human ESC/iPSC

(A and B) Immunofluorescence staining for early forebrain primordium markers Nestin/Pax6 (A) and Nestin/Otx1/2 (B), after 19 days of differentiation.

(legend continued on next page)

electrophysiological properties of the cell population, with increased proportion of cells displaying induced repetitive firing and spontaneous synaptic currents (excitatory postsynaptic currents [EPSCs]) and, conversely, a reduced proportion of cells showing immature induced single action potentials (Figures 1L–1N, Figure S4, and Table S1). At the single cell level, we also observed an increase in the intensity of the voltage-dependent sodium current and in the amplitude of action potentials (Figures S4B–S4E and Table S1).

Altogether, these data demonstrate that human ESC-derived neurons gradually acquire in vitro all characteristic functional and morphological features of cortical pyramidal neurons.

A Species-Specific Sequence of Generation of Pyramidal Neurons of Diverse Layer Identities

Pyramidal neurons can be further subdivided by a repertoire of molecular markers identifying layer-specific neuronal populations (Gaspard and Vanderhaeghen, 2011; Molyneaux et al., 2007) (Figure 2J). Neurons from different layers are generated at distinct time points, where the earliest-born neurons generated in the cortex are pioneer neurons, followed by deep cortical layers VI and V, then by upper layers IV, and lastly layers II/III. To test whether a similar process occurred during corticogenesis from human ESCs, we determined the timing of onset of expression of layer-specific markers during the course of differentiation. The first neurons generated appeared around days 10–16 in culture (less than 1% of all cells) (Figure 2I, Figure S5P) and were positive for TBR1, calretinin, and reelin (markers of pioneer and Cajal-Retzius neurons) (Figures 2A, 2B, and 2I–2K). Later on, from around 40 DIV (a stage where 40% of the cells are neurons) (Figure 2I, Figure S5P), the proportion of TBR1-positive neurons kept increasing, while the proportion of calretinin neurons tended to decrease steadily (Figure 2I), suggesting that the majority of TBR1-positive/calretinin-negative neurons correspond to deep layer neurons VI and V (Figures 2I and 2J). This was consistent with the appearance of FOXP2-positive and TBR1/CTIP2 double-positive neurons (layer VI) (Figures 2C, 2I, and 2J, Figures S6A–S6F) at 24–28 DIV, followed by CTIP2-positive neurons (layer V) at 37 DIV (Figures 2D and 2I–2K). Finally, SATB2-positive neurons, corresponding to callosal neurons from layers V and upper layer neurons, and CUX1/BRN2-positive neurons, corresponding to upper layer neurons, started to appear at the latest time points in culture (61–72 DIV) (Figures 2E–2G and 2I–2K). In addition, deep layer marker genes like FOXP1 and ETV1 were expressed from day 16 and displayed reduced expression from 61 DIV, at the onset of upper layer neuron generation (Figure 2K). Notably, there appeared to be a preferential bias toward the generation of deep layer fated neurons in the system, while upper layer neurons remained at low levels compared with the cortex generated in vivo, similarly to what we previously found during mouse ESC-derived corticogenesis (Gaspard et al., 2008).

Several other ESC and iPSC lines displayed a similar temporal pattern of neurogenesis, resulting in a comparable repertoire of neurons displaying diverse layer-specific patterns of identity (Figures S6G–S6K).

The repertoire of neuronal identity was further examined at a broader level using microarray profiling, focusing on 78 previously documented layer-specific genes (Bedogni et al., 2010; Molyneaux et al., 2007; Zeng et al., 2010). This revealed that most layer-specific genes were upregulated during hESC-corticogenesis, and their overall pattern appeared to be intermediate between those observed for human cortex samples at 9 and 19 GW, corresponding to most deep layer and a fraction of upper layer markers (Figure S7).

Corticogenesis from human ESC/iPSC thus follows a similar temporal sequence as from mouse ESC (Gaspard et al., 2008), but it extends over a period of time that is much more protracted (over 80 DIV instead of 20), strongly reminiscent of the extended timing of corticogenesis occurring in vivo in the human species

(C) qRT-PCR analysis of human ESC-derived neural progenitors in culture. Data are shown as relative amount of mRNA compared to the values at day 5 of differentiation, as value 1 ± SEM (fold change) (n = 3–7).
(D) qRT-PCR analysis of the ESC-derived progenitors at day 19 of differentiation, after 8 or 16 days of treatment with noggin. Data are shown as relative amount of mRNA compared to the values of noggin 0–8 treatment, as value 1 ± SEM (fold change) (n = 3).
(E) Top: quantification of the proportion of ßIII-tubulin-positive neurons expressing VGlut1 (days 44 and 72), VGAT (day 44), GAD67 (day 44), TH (day 44), and ChAT (day 44). Mean ± SEM (n = 2 experiments). Bottom: qRT-PCR analysis of the expression of Vglut1 and Vglut2 after 24, 44, 61, and 72 days of differentiation. Data are shown as relative amount of mRNA compared to the values of day 24, as value 1 ± SEM (fold change) (n = 3).
(F) Top: proportion of neurons displaying a pyramidal morphology index (PMI) above the cutoff of 1.2. Mean ± SEM (n = 3). Bottom: proportion of neurons displaying pyramidal, bipolar, or multipolar morphology. Mean ± SEM (n = 3 experiments).
(G) Immunofluorescence of ESC-derived neurons expressing MAP2 at day 72.
(H) Immunofluorescence staining of ESC-derived neurons after 72 days of differentiation for ßIII-tubulin (in green) and VGlut1 (in red). Magnification view of VGlut1 is depicted on the right bottom corner.
(I and J) Immunofluorescence staining at day 82 of ESC-derived neurons for ßIII-tubulin (in green) and synaptophysin (in red) (I) and HOMER1 (in red) (J). Magnification views of Syn and Homer1 are depicted on the right bottom corner.
(K) Heatmap analysis showing the normalized expression of pyramidal neuronal maturation genes in two samples of undifferentiated H9 ESC at day 0 (s1, s2), two sets of cells differentiated for 24, 44, and 61–72 DIV (s1, s2), and two samples from human embryonic cortex at 9 and 19 gestational weeks (9/19 GW) (s1, s2). Top: legend showing color code for comparative levels of expression.
(L) Representative traces of evoked (left) and spontaneous (right) action potentials from current-clamp recordings in ESC-derived neurons after 50–60 days of differentiation.
(M) Two examples of excitatory spontaneous synaptic currents (EPSCs) recorded in ESC-derived neurons after 50 days in culture, inhibited by the application of APV and CNQX (right, below) (NMDA and AMPA receptor antagonists).
(N) Graph showing the proportion of cells displaying EPSCs, spontaneous AP, induced single AP, and repetitive AP among cells with Na current at days 38–65 and days 68–82. Mean ± standard error of the proportion (SEP) (days 38–65 n = 61, days 68–82 n = 16) (t test, ***$p < 0.001$, *$p < 0.05$). Scale bars represent 50 μm in (A and B) and in left of (H–J) and 25 μm in right of (H–J).

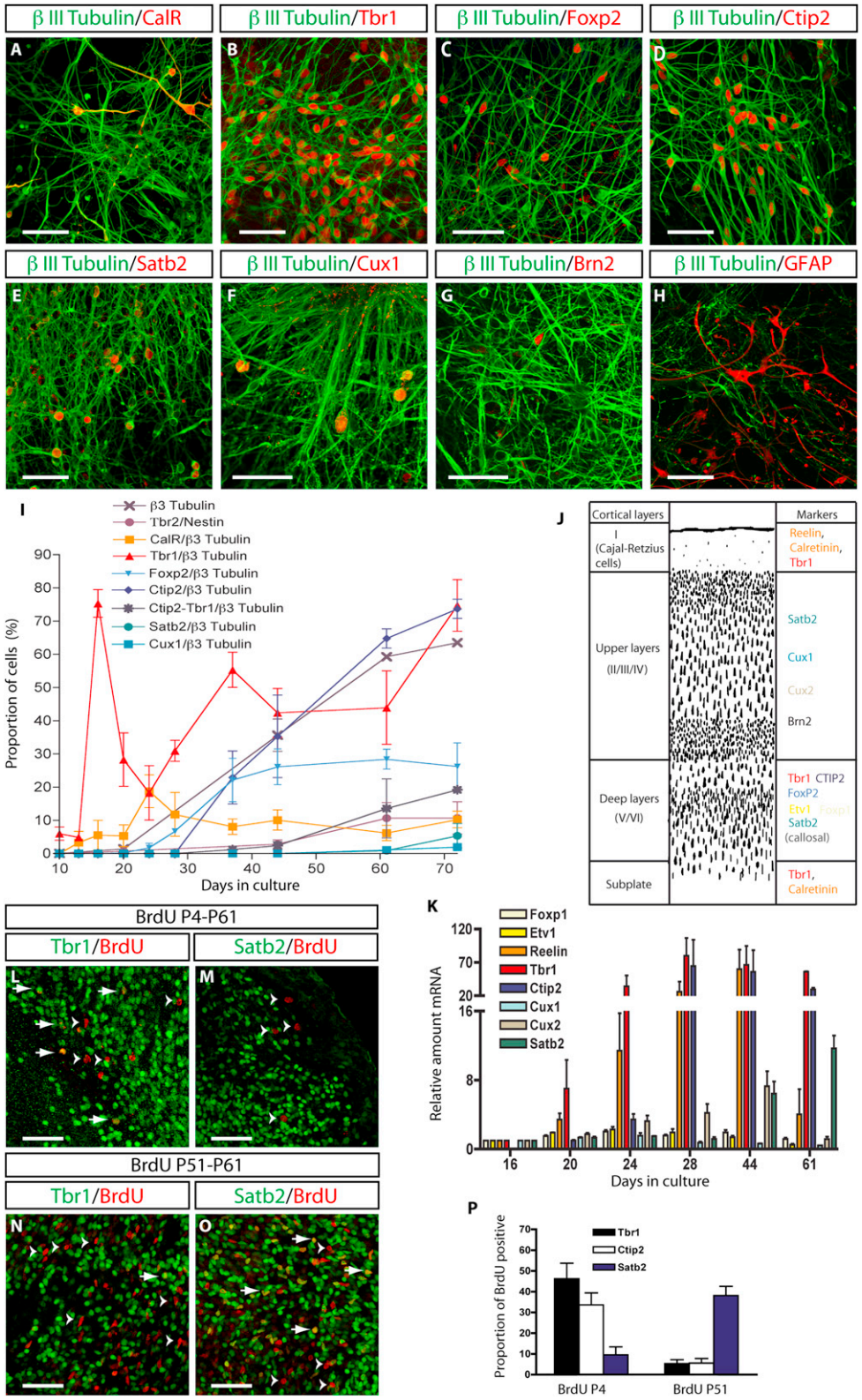

Figure 2. Sequential Generation of Human Pyramidal Neurons of Diverse Layer Identities In Vitro and after In Vivo Grafting

(A–I) A repertoire of distinct cortical neuronal and nonneuronal subtypes present after 72–82 days of differentiation. Markers (in red) calretinin (CalR) (A), TBR1 (B), FOXP2 (C), CTIP2 (D), SATB2 (E), CUX1 (F), and BRN2 (G) are all present in a proportion of ßIII-tubulin neurons (in green).

(legend continued on next page)

(Lui et al., 2011; Rakic, 1995). To test further the significance of these observations, we compared directly mouse and human ESC corticogenesis in identical conditions. Mouse and human ESC were cultured following the protocol optimized for human cells, both in the presence of cyclopamine to allow full dorsal specification of the mouse ESC-derived progenitors (Gaspard et al., 2008) (while cyclopamine was found to have no effect in the human system; Figure S3). Whereas the identity of early cortical progenitors was comparable between mouse and human at early and later stages (Figures S5A–S5C and data not shown), the appearance of BLBP-positive neurogenic radial glial cells and neurons were much delayed in the human cultures (Figures S5D–S5I and S5P). Moreover, while mouse cortical neurons of all layer identities were generated sequentially over 20 DIV, at the same stage only early pioneer TBR1-positive neurons could be detected from human ESC (Figures S5J–S5O). Overall these data indicate that in vitro cortical neurogenesis from human pluripotent stem cells is delayed and prolonged when compared to the mouse, thus mimicking the prolonged timeline of human corticogenesis (Lui et al., 2011; Rakic, 1995).

Human ESC-Derived Cortical Cells Engraft Robustly and Mature Following a Species-Specific Timeline in Mouse Newborn Cortex

The identity of a neuron is best attested by its hodological properties, and this is particularly important for cortical neurons, which display distinct patterns of axonal projections depending on their layer and/or areal identity.

To test this prominent aspect of cortical neuronal identity, we undertook grafting experiments in neonatal mice, a well-characterized paradigm to assess the hodological properties of projection neurons (Gaillard et al., 1998). For this purpose, we generated a human ESC line expressing green fluorescent protein (GFP) ubiquitously. GFP-positive hESCs were first differentiated into cortical-like cells for 24 DIV, then grafted into the frontal cortex of mouse neonates, and analyzed after up to 9/10 months posttransplantation (mpt).

Most of the grafts were located underneath or within the frontal cortex, with most of the GFP-positive cells remaining confined within the graft (Figures 3A and 4A). No evidence for teratoma formation was found 6–9 mpt (data not shown). Importantly, the human GFP-positive cells expressed in all cases a specific human nuclear antigen and showed no evidence of graft-to-host fusion (such as binucleated GFP cells) (Figures S8A–S8C).

The grafts mainly consisted of neurons, as shown by the GFP/ßIII-tubulin double-positive cells at 1/2 mpt and GFP/MAP2 at 6 mpt (Figures S8D–S8I, S9A and S9B), with some Nestin-positive progenitors still present at 1–2 mpt (data not shown). The grafted neurons were positive for the telencephalic marker FOXG1 (Figures S9A and S9B) and displayed appropriate molecular markers corresponding to cortical pyramidal neurons of different layer identities (Figure S9). This led us to test whether the temporal pattern observed in vitro was also present after in vivo grafting. We first observed that, while markers corresponding to deep layer neurons (TBR1, FOXP2, and CTIP2) could be readily detected after 1 mpt, the upper layer marker SATB2 was detectable in grafted neurons only at 2 mpt (Figures S9A and S9B). We next performed BrdU nuclear labeling experiments in the grafted mice to determine the date of birth of neurons of distinct layer identity. This analysis revealed that BrdU-labeled neurons that were born early (4 days after grafting) corresponded mostly to TBR1- or CTIP2-positive deep layer neurons, while those born later (51 days after grafting) corresponded mostly to SATB2-positive callosal and/or upper layer neurons (Figures 2L–2P). In addition, we found significant coexpression of TBR1 and CTIP2 (as found in vivo; McKenna et al., 2011) (Figures S6E and S6F) but largely mutually exclusive expression of SATB2 and CTIP2 in the human ESC-derived transplanted neurons (as found in vivo; Alcamo et al., 2008), further indicating that distinct cortical neuron populations are generated sequentially, even after in vivo transplantation into the mouse (Figures S9C and S9D).

Human ESC-Derived Cortical Neurons Project to Layer-Specific Targets

We next examined the axonal projections of the grafted neurons after 1–6 months and compared them with known endogenous patterns of projection of native cortical projection neurons. GFP-positive fibers were detected along the external capsule and corpus callosum, up to the ipsilateral and contralateral cortex (Figures 3A, 3C, and 3F and 4A and 4B). GFP-positive axons corresponding to subcortical projections were also detected along the internal capsule and cerebral peduncles and reached subcortical targets in the striatum, thalamus, midbrain, and hindbrain (Figures 3A, 3B, 3D, 3E, 3G, and 3H and 4A and 4C–4F). The pattern of axonal projections was cortex specific, i.e., graft-derived axons did not significantly innervate brain regions that are not targets of cortical neurons, such as substantia nigra or cerebellar structures (Figure 4M). Moreover, it confirmed the presence of neurons of diverse layer identities within the grafted cells, with projections to the thalamus (target of layer VI), striatum, midbrain/hindbrain (targets of layer V), and ipsi- as well as contralateral cortex (targets of layer II/III/V) (Figures 3 and 4).

(H) Immunodetection of astrocytes expressing GFAP (in red) and neurons expressing ßIII-tubulin (in green) after 82 days of differentiation.
(I) Time course of the proportion of cells expressing markers of progenitors (TBR2), neurons (ßIII-tubulin), and different layer-specific markers among the neurons after ESC differentiation. Mean ± SEM (n = 2–4 experiments).
(J) Scheme depicting patterns of the layer-specific markers in vivo.
(K) qRT-PCR analysis showing the evolution in time of the expression of layer-specific markers. Data are shown as relative amount of mRNA compared to the values of day 16 as value 1 ± SEM (fold change) (n = 2–4).
(L–O) Immunofluorescence images of BrdU-labeled cells (in red) and Tbr1 (in green) (L and N) or Satb2 (in green) (M and O) in mice BrdU injected at P4 and analyzed at P61 (L and M) or BrdU injected at P51 and analyzed at P61 (N and O). Arrows show colocalization of the two markers, and arrowheads show cells expressing only BrdU.
(P) Quantification of the proportion of Tbr1-, CTIP2-, or Satb2-positive cells among the BrdU-positive population 61 days after grafting, pulse chased 4 or 51 days after grafting. Mean ± SEM (n = 80–100 neurons). Scale bars represent 50 μm.

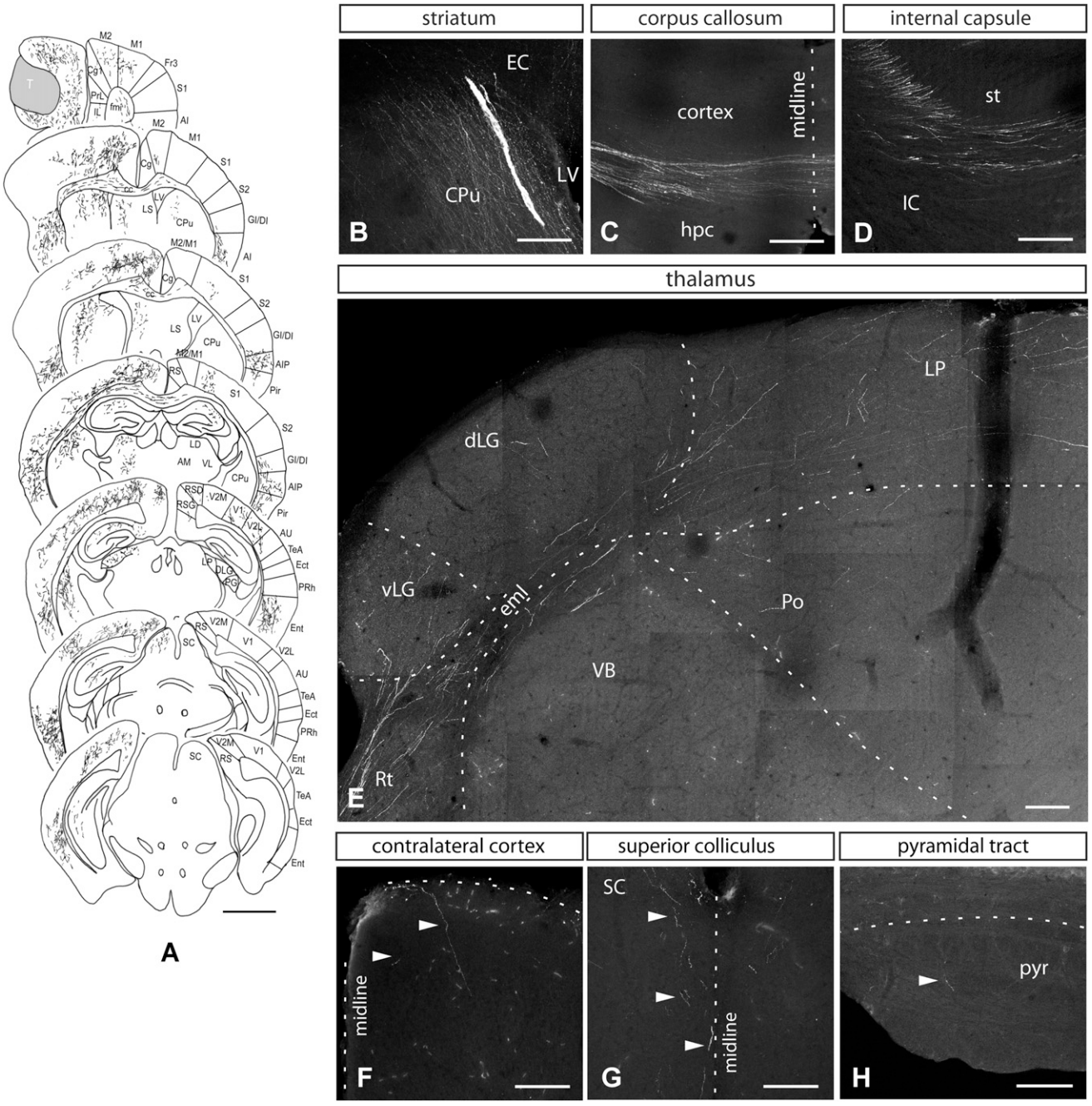

Figure 3. Human ESC-Derived Cortical Neurons Integrate and Send Cortical-like Axonal Projections after Grafting in Newborn Mouse Cortex

(A) Camera lucida drawing of the pattern of axonal projections 2 months after grafting. T, transplant. Abbreviations according to Paxinos and Franklin (1997).

(B–H) GFP-positive axonal projections detected by immunofluorescence in various brain structures 2 months after grafting. Fibers in the striatum (CPu) (B), corpus callosum (C), and internal capsule (IC) (D).

(E) Fibers enter the thalamus via the reticulate thalamus (Rt) and reach the ventral lateral geniculate (vLG), dorsal lateral geniculate (dLG), and lateroposterior nuclei (LP) and, to a lesser extent, the ventrobasal/-posterior (VB) and posterior (Po) nuclei. eml, external medullary lamina.

(F–H) Fibers in the contralateral cortex (F), superior colliculus (SC) (G), and the pyramidal tract (Pyr) (H). EC, external capsule; hpc, hippocampus; IC, internal capsule; LV, lateral ventricle; st, stria terminalis. Scale bars represent 2 mm in (A) and 100 μm in (B–H).

Quantification of the projections at 1–6 months revealed an increase in the percentage of animals with far-reaching projections (in the midbrain and hindbrain including the pyramidal tract) (Figure S8L), as well as in the number of total axonal projections (Figures 4G–4J). Interestingly, the latter was most prominent when examining targets of late-generated neurons,

such as the striatum, midbrain/hindbrain (target of layer V), and contralateral cortex (target of layers II/III/V) (Figures 4G–4J). This time-dependent pattern of axonal projections is consistent with the sequential generation of these neurons, observed in vitro and in vivo from human ESC.

Finally, we looked at the direct relationship between patterns of axonal projections and expression of selective transcription factors, a striking feature of cortical projections neurons (Molyneaux et al., 2007). For instance, CTIP2-positive neurons mostly correspond to layer V corticofugal neurons that target the midbrain, hindbrain, and spinal cord, while layer VI TBR1-positive neurons project mostly to the thalamus. We performed retrograde tracing experiments in animals 9 months after grafting, targeting the thalamus or the midbrain superior colliculus, combined with immunostaining of the retrogradely labeled grafted neurons, and compared their patterns with those of the host cortical neurons (Figure 5). Remarkably, this revealed that most (70%) of the grafted neurons retrogradely labeled from the thalamus were found to be TBR1 positive, while fewer (<30%) were CTIP2 positive, like layer VI host neurons (Figures 5A–5E). In contrast, most (>80%) of the grafted neurons that were retrogradely labeled from the midbrain were CTIP2 positive, while fewer (<35%) were TBR1 positive, as was observed for layer V host neurons (Figures 5A, 5B, and 5F–5H). While these data confirm the robustness of the axonal patterns of the grafted neurons, they also indicate that the expression of specific transcription factors is correlated with patterns of axonal projections of the grafted neurons, as for genuine cortical projection neurons.

Human ESC-Derived Cortical Neurons Project to Area-Specific Targets

We next examined the areal specificity of axonal projections, whereby projection neurons of distinct areas target diverse brain structures, such as visual nuclei for the visual cortex or pyramidal tract for motor cortex. Similar grafting experiments with mouse ESC-derived cortical neurons revealed specific patterns of projections, corresponding mostly to visual and limbic identity (Gaspard et al., 2008). Interestingly, quantitative examination of the human graft-derived axonal projections 2 mpt revealed a pattern that was also indicative of visual or limbic identity, with projections to visual and limbic targets in the thalamus (LG/LP/LD), dorsomedial (DM) striatum, and midbrain (SC/PAG) (Figures 3 and 4G–4L). However, at 6 mpt, the projections displayed a much broader pattern of areal identity, with axons reaching motor targets such as dorsolateral striatum (DL) and the pyramidal tract or somatosensory targets such as the somatosensory VB and Po nuclei (thalamus) (Figures 4A–4L). Consistent with a broader pattern of cortical areal identity at later stages, the visual or limbic cortex marker COUP-TFI was prominently expressed among the grafted neurons at 2 mpt but was much less prevalent in later generated neurons at 6–9 mpt (Figures S8J and S8K).

Human ESC-Derived Neurons Display Elaborate Patterns of Dendritic Outgrowth and Synaptogenesis

Pyramidal neurons also display specific patterns of dendritic orientation, growth, and targeting (Barnes and Polleux, 2009). This important aspect of maturation and complexity could not be addressed for the majority of neurons, located within the bulk of the graft. However, in every case examined, a small number of neurons could be found outside of the graft, many of which had settled within the host cortex (Figure 6). Most of these neurons displayed a pyramidal morphology, with one larger apical dendrite oriented radially within the cortex (Figures 6A and 6B). When examined from 3 weeks to 2 mpt, they displayed relatively simple and immature patterns of dendritic growth (Figures 6A–6D). However, this pattern complexified dramatically with time (Figures 6A–6F), and at 9 mpt most neurons examined displayed elaborate dendritic growth and branching, highly reminiscent of mature pyramidal neurons (Figures 6F and 6G). Moreover, closer inspection of the dendrites revealed the presence of numerous dendritic spines (Figure 6H), suggesting that active synaptogenesis had taken place. Indeed, markers of glutamatergic neurons and pre- and postsynaptic components were abundantly detected in the graft (Figures 7A–7C). Electron microscopy combined with GFP immunolabeling confirmed the presence of numerous synapses from the grafted neurons to the host after 6 months, including at subcortical targets (Figures 7D–7F). Reciprocal synapses from the host to the grafted neurons were also observed (Figure 7G), and innervation of the graft by the host thalamus was confirmed by anterograde tracing (Figure 7I). This analysis also revealed GFP-positive fibers myelinated by the host, providing further indication of full integration in the host brain (Figure 7H).

Human ESC-Derived Neurons Are Functionally Integrated into the Mouse Cortical Microcircuitry

We then analyzed the functionality of human ESC-derived neurons integrated into the mouse cortex, using patch-clamp recordings on ex vivo brain slices acutely obtained from transplanted mice at 9 mpt (Figure 8). Strikingly, we found that all human neurons examined (n = 9, from 3 transplanted mice) displayed passive membrane properties and excitability typical of mature cortical neurons, with most of them (n = 8/9) displaying a regular accommodating firing pattern, characteristic of pyramidal neurons (Figures 8A–8C) (McCormick et al., 1985). We next assessed the incoming synaptic connectivity of the transplanted neurons. We first observed that all recorded neurons displayed at rest consistent spontaneous synaptic potential (PSP) occurrence, which could be blocked by glutamatergic receptor antagonists (CNQX and AP-V) (Figures 8D–8F), indicating the integration of ESC-derived neurons into glutamatergic circuits (Figures 8D–8F). Moreover and most strikingly, we tested the evoked responsiveness of the transplanted human neurons upon a train of extracellular electrical stimulations at a distance of the graft within the mouse host cortex. This evoked robust synaptic responses in all tested neurons that corresponded to glutamatergic and GABA-ergic inputs (Figures 8G and 8H), with short-term plasticity profiles common in cortical microcircuits (Reyes and Sakmann, 1999; Wang et al., 2006).

DISCUSSION

The mechanisms underlying human cortex development have major implications in neurobiology and neurology, but their study

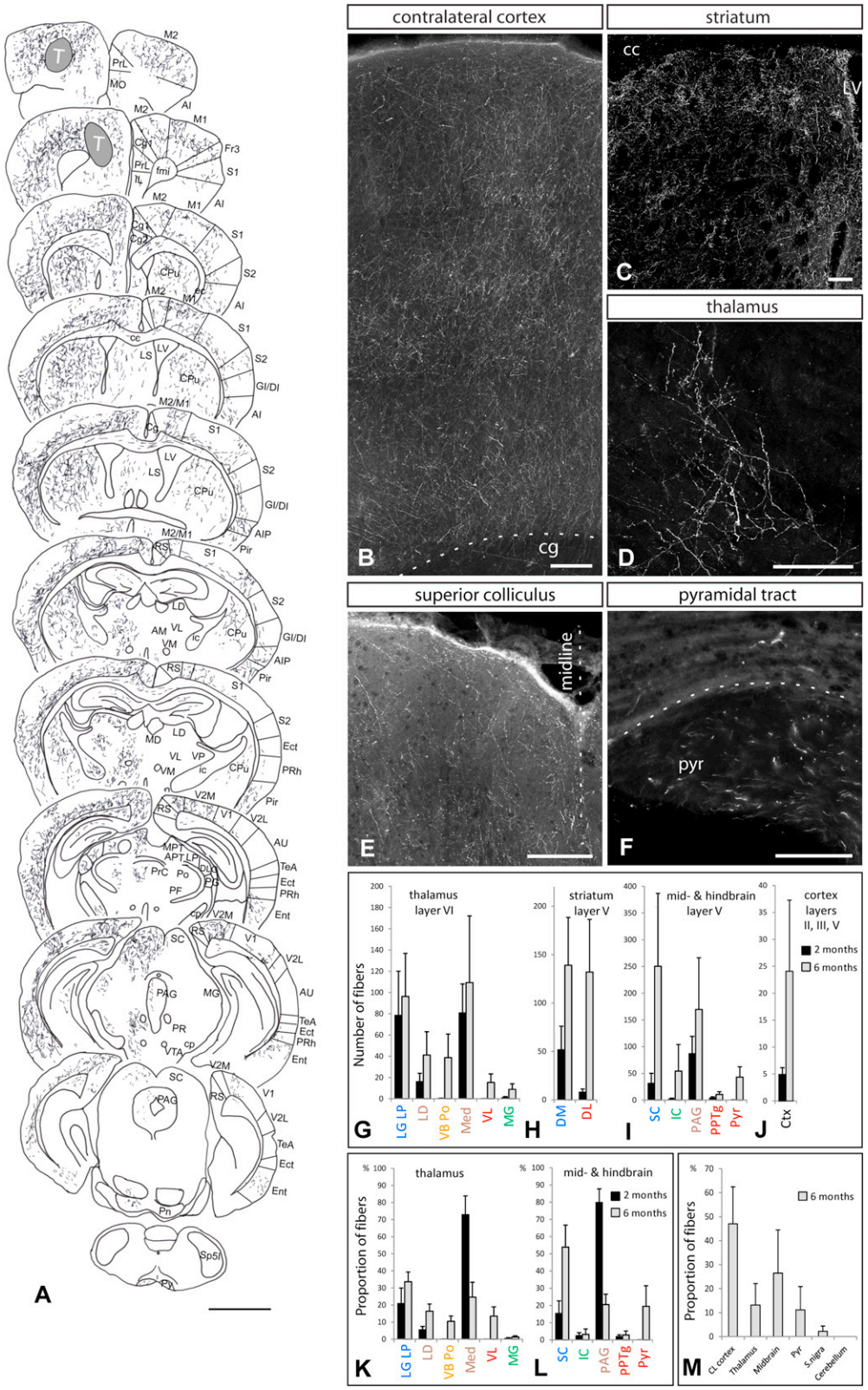

Figure 4. Maturation of the Pattern of Axonal Projections of ESC-Derived Neurons

(A) Camera lucida drawing of the pattern of axonal projections 6 months after grafting. T, transplant. Abbreviations according to Paxinos and Franklin (1997).

(legend continued on next page)

has remained difficult due to limited experimental accessibility to human fetal brain material. Here, we show that human corticogenesis from ESC and iPSC leads to a collection of functional neurons that display most salient features of native pyramidal neurons, including gene expression, morphology, physiology, and, most importantly, hodological properties assessed in vivo by robust and specific patterns of axonal and dendritic outgrowth and functional synaptic integration in the host circuitry.

The generation of cortical-like neurons was previously reported from human ESC and iPSC (Eiraku et al., 2008; Li et al., 2009; Shi et al., 2012; Zeng et al., 2010). However, since these protocols used cell aggregate cultures and/or added morphogens, it had remained unclear whether the intrinsic pathway uncovered in mouse (Gaspard et al., 2008) was conserved in human cells. Here, we report the robust differentiation of human ESC and iPSC into cortical neurons, following a monoadherent culture condition in a chemically defined medium devoid of added morphogens. While these data indicate that the absence of morphogens appears to be critical for both mouse and human ESC corticogenesis, there are also interesting and important differences between the two species, such as the required use of SHH antagonists in the mouse and of BMP antagonists in the human cells. In addition and most strikingly, the two systems differ greatly by their temporal appearance, which could be reminiscent of the in vivo temporal differences between the two species.

A highly conserved feature of cortical neuron specification is temporal patterning, whereby neurons of distinct layer identity are generated sequentially (Gaspard and Vanderhaeghen, 2011; Leone et al., 2008; Molyneaux et al., 2007; Okano and Temple, 2009). We observed a similar temporal patterning from human ESC and iPSC in vitro and, most strikingly, even after intracerebral grafting in vivo. Notably, like in the mouse ESC-derived corticogenesis, most of the pyramidal neurons generated here in vitro display an identity corresponding to deep layers, while upper layer neurons are underrepresented when compared to the in vivo situation. This contrasts with a recent report describing the generation of deep and upper layer neurons in equivalent proportions, from human ESC cultured in the presence of retinoic acid precursors (Shi et al., 2012). Moreover, we observed a higher proportion of upper layer neurons after transplantation than after purely in vitro conditions, while the generation of deep layer neurons appeared to be similarly efficient in vitro and in vivo. Overall, this could suggest that extrinsic cues, which are not added in our minimum culture conditions and might be present in the neonatal mouse cortex, may be required for proper upper layer neuron specification.

The identity of cortical neurons can be best attested by their hodological properties, such as their patterns of axonal and dendritic projections. Our grafting experiments revealed robust and specific axon targeting to brain regions normally innervated by cortical neurons, as well as dendritic patterns corresponding to those of native pyramidal neurons, including the presence of dendritic spines. In addition, the grafted neurons appeared to correspond to a diverse repertoire of cortical neurons, as assessed by their pattern of axonal projections that corresponded to all cortical layers, which could be correlated with layer-specific gene expression. These data reveal a robust correlation between molecular and hodological properties of the grafted neurons, even for noncortical or mouse cells.

On the other hand, human ESC-derived cortical neurons displayed area-specific patterns of projections. We previously found that mouse ESC-derived neurons displayed specific patterns of axonal projections corresponding to visual and limbic occipital cortex (Gaspard et al., 2008). A similar axonal pattern was observed with human cortical cells 2 months after grafting, suggesting that in vitro corticogenesis can lead to occipital areal identity also in human cells. However, unlike in the mouse, after longer periods the axonal projections corresponded to a wider range of areal identities, including motor and somatosensory. These data suggest that specific patterns of visual or limbic areal identity may be acquired during in vitro differentiation from human ESC, like in the mouse, but that after grafting a substantial fraction of the cells can be specified to other areal identities over time, perhaps in relation with their earlier stage of maturation at the time of grafting. In support of this hypothesis, most of the grafted neurons expressed the occipital cortex marker COUP-TFI after 2 months, whereas far fewer neurons were found to be positive after 6–9 months. This is highly reminiscent of the data obtained with rodent native or ESC-derived cortical cells, which show different patterns of areal fate specification depending on their degree of commitment and maturation at the time of grafting (Hansen et al., 2011; Ideguchi et al., 2010; Pinaudeau et al., 2000). It will be interesting in the future to further test these issues, by characterizing the molecular areal identity of the transplanted neurons over time and by assessing the areal patterns of projections of ESC-derived cells differentiated for a longer time prior to transplantation and/or after transplantation into other areas, such as somatosensory or visual cortex.

(B–F) GFP-positive fibers detected within the contralateral cortex (B), striatum (C), thalamus (D), superior colliculus (E), and pyramidal tract (pyr) (F).
(G–J) Quantification of the distribution of GFP-positive fibers to the layer VI target thalamus (G), layer V target striatum (H), layer V target midbrain/hindbrain (I), and layer II/III/V target contraleteral cortex (J) after 2 and 6 months. n = 12 for 2 months, n = 6 for 6 months. Medium values are given ±SEM.
(K and L) Proportion of fibers within the different structures of the thalamus and mid/hindbrain after 2 and 6 months. n = 12 for 2 months, n = 6 for 6 months. Medium values are given ±SEM, x axis color code refers to the areal specificity of innervation of each target examined: visual, blue; limbic, brown; somatosensory, orange; motor, red; auditory, green. LG, lateral geniculate; LP, lateroposterior; LD, laterodorsal; VB, ventrobasal; Po, posterior; Med, medial; VL, ventrolateral; MG, medial geniculate nuclei of the thalamus; DM, dorsomedial; DL, dorsolateral parts of the striatum; SC, superior colliculus; IC, inferior colliculus; PAG, periaqueductal gray matter; PPTg, pedunculopontine nucleus; Pyr, pyramidal tract.
(M) Quantification of the proportional distribution of GFP-positive fibers within cortical targets: contralateral cortex (CL cortex), thalamus (LG, LP, LD, VB, Po, Med, VL, MG), midbrain (SC, IC, PAG, PPTg), and pyramidal tract (Pyr), and within noncortical targets: substantia nigra (s. nigra) and cerebellum after 6 months. n = 6. Medium values are given ±SEM. Scale bars represent 2 mm in (A) and 100 μm in (B–F).

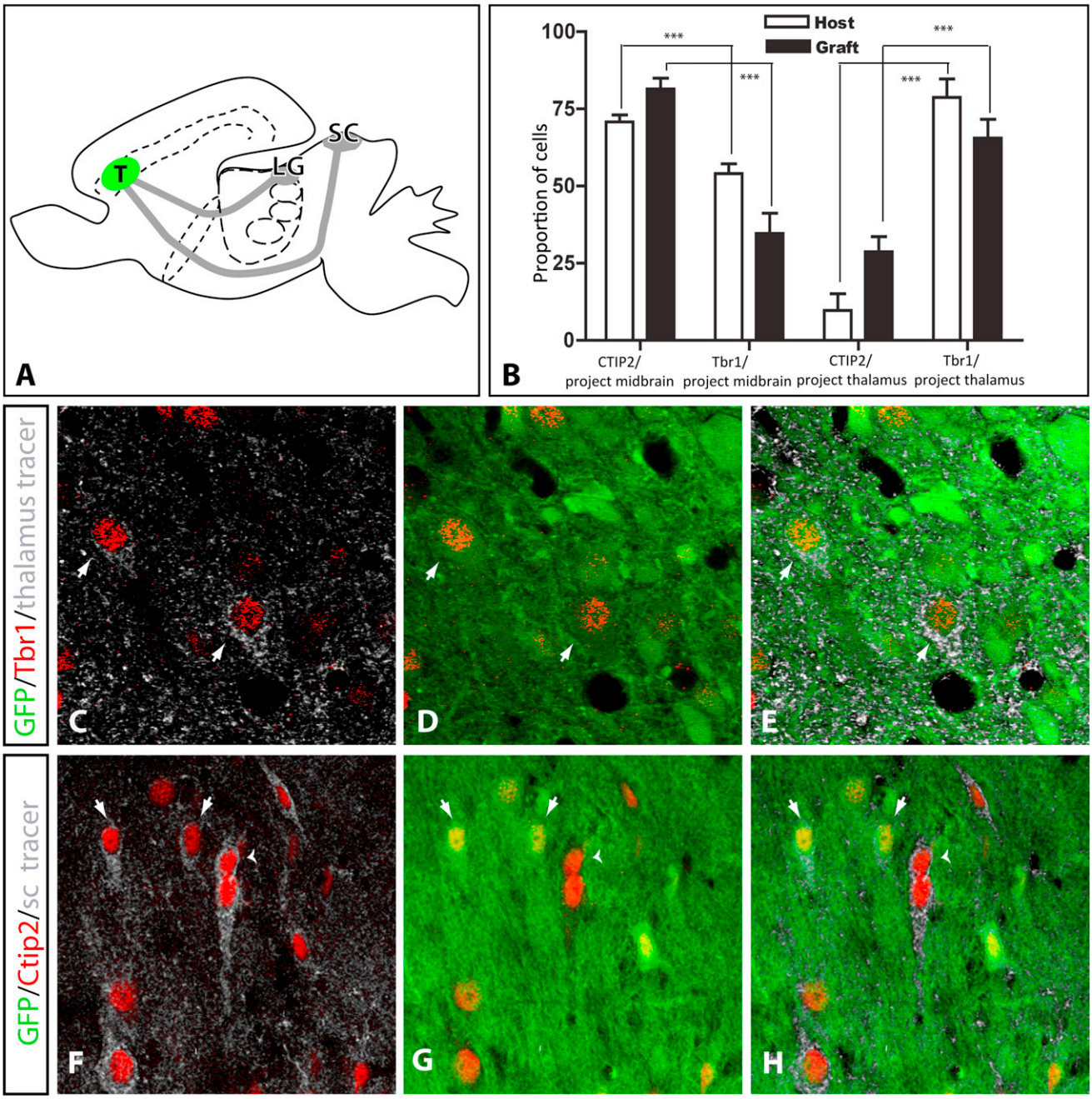

Figure 5. Human ESC-Derived Cortical Neurons Display Coordinated Patterns of Axonal Projections and Molecular Identity

(A) Cartoon depicting experiments of retrograde tracing injections in the thalamus (LG) or in the midbrain (SC). T, transplant.

(B) Quantification of the percentage of Ctip2- or Tbr1-positive host and grafted cells among all cells labeled with the midbrain or the thalamic retrograde tracer. ($n > 30$ cells). Values are expressed as the mean ± SEP (z test, ***$p < 0.001$).

(C–E) Thalamic injection of a retrograde tracer labels Tbr1 and GFP double-positive grafted hESC-derived neurons. Immunostaining of GFP (in green) (D and E), Tbr1 (in red) (C and E), and the retrograde tracer (in gray) (C and E). Arrows show hESC-derived neurons positive for GFP/Tbr1 and the retrograde tracer.

(F–H) Superior colliculus (midbrain) injection of a retrograde tracer labels CTIP2 and GFP double-positive hESC-derived neurons. Immunostaining of GFP (in green) (G and H), CTIP2 (in red) (F–H), and the retrograde tracer (in gray) (F and H). Arrows show hESC-derived neurons positive for GFP/CTIP2 and the retrograde tracer; arrowhead shows a host-derived neuron, negative for GFP and positive for CTIP2 and the retrograde tracer.

Our data constitute direct in vivo demonstration of cortical identity of neurons differentiated from human ESC. Most importantly, the robustness and extent of the process of integration and differentiation of the grafted neurons reveals the possibility to combine human ESC/iPSC corticogenesis with xenografting for the in vivo modeling of human cortical diseases. This

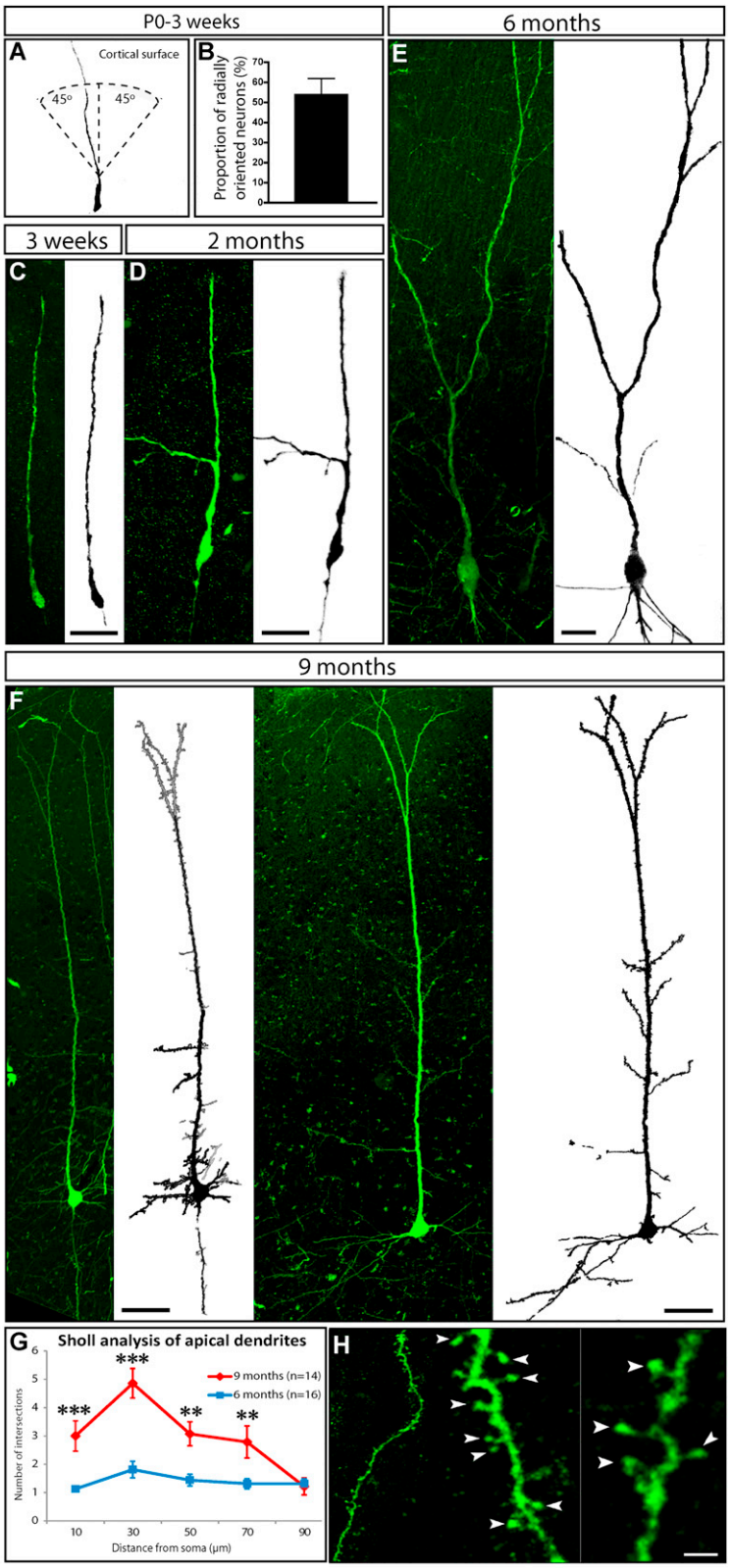

Figure 6. Human ESC-Derived Cortical Neurons Undergo Elaborate Dendritic Maturation after 9 Months Grafted In Vivo

(A) Camera lucida image representing a human ESC-derived neuron in the cortex extending its apical dendrite toward the cortical surface 3 weeks after grafting.

(B) Quantification of the percentage of neurons displaying an apical dendrite oriented toward the cortical surface after 3 weeks. Mean ± SEM (n = 102 neurons).

(C–E) Representative confocal and camera lucida images of grafted human GFP-positive neurons with characteristic immature dendritic patterns 3 weeks and 2 and 6 months after grafting.

(F) Two examples of hESC-derived neurons (GFP-positive) displaying a more mature and elaborate dendritic pattern.

(G) Quantification of the Sholl analysis performed in apical dendrites of hESC-derived neurons after 6 and 9 months grafting. n = 16 for 6 months and n = 14 for 9 months. $^{**}p < 0.01$, $^{***}p < 0.001$.

(H) GFP immunostaining revealing dendritic spines on grafted neurons. Scale bars represent 20 μm in (C–G) and 5 μm in (H).

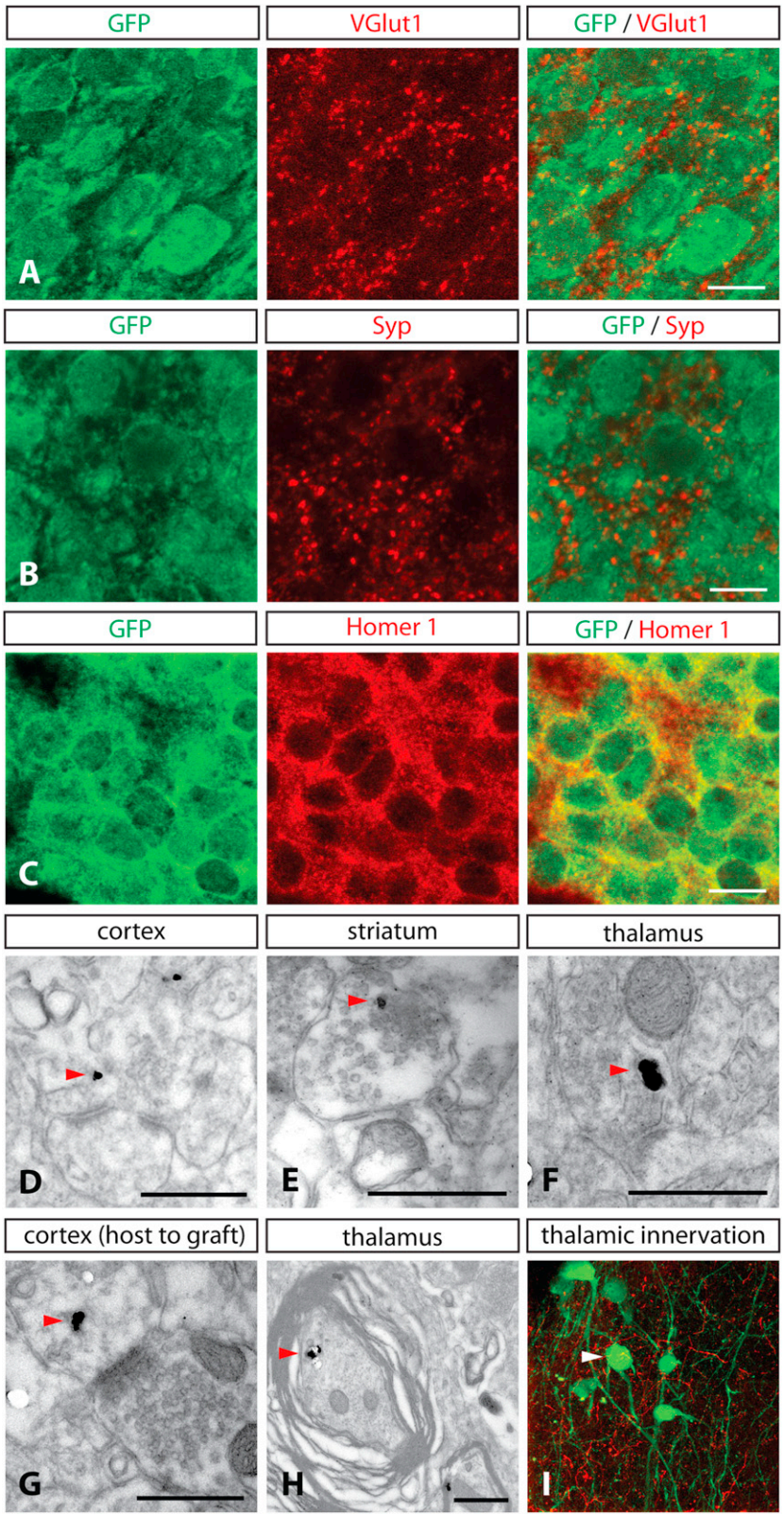

Figure 7. Grafted Human ESC-Derived Neurons Establish Reciprocal Synapses with the Host and Receive Thalamic Input

(A–C) Immunofluorescence images from 2-month-old grafts showing the expression of GFP (in green) and VGlut1 (in red) (A), synaptophysin (Syp) (in red) (B), and HOMER1 (in red) (C).

(D–F) Electron microscopy combined with GFP immunostaining (red arrowheads) of synaptic contacts from graft to host within the cortex (D), striatum (E), and thalamus (F), and from host to graft (G) 6 months after grafting.

(H) Electron microscopy image of GFP-positive myelinated fibers within the thalamus 6 months after grafting. Red arrowheads show GFP immunogold detection.

(I) Fibers positive for the anterograde tracer BDA (in red) were detected in close vicinity of GFP-positive grafted neurons (in green) after thalamic BDA injection 6 months after grafting. Scale bars represent 10 μm in (A–C) and 500 nm in (D–H).

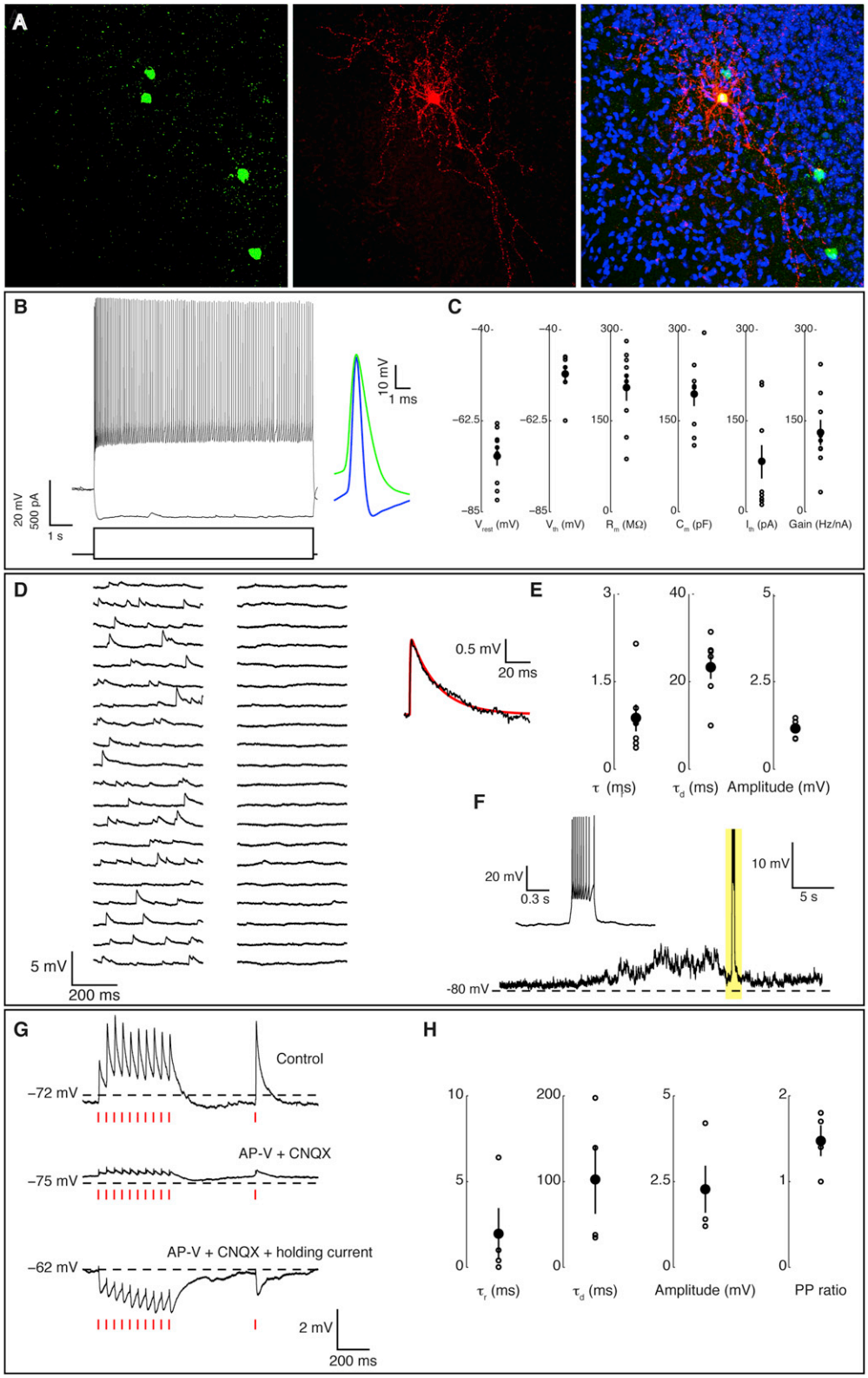

Figure 8. Grafted Human ESC-Derived Neurons Integrate Functionally in the Synaptic Microcircuitry of the Mouse Host Brain

(A) Immunofluorescence staining showing human GFP-positive neurons (in green) (left and right) integrated into the mouse cortex and stained for biocytin (in red, injected during patch-clamp recording) (middle and right) and Hoechst (in blue) (right).

(legend continued on next page)

approach could be particularly insightful to study neurodevelopmental conditions of genetic origin that affect complex patterns of morphology and connectivity of cortical neurons, and for which animal or purely in vitro models may be insufficient (Dolmetsch and Geschwind, 2011; Han et al., 2011; Marchetto et al., 2010; Zhang et al., 2010). In addition, it will be interesting to test whether and how ESC-/iPSC-derived cortical cells could be used in cell therapy paradigms for lesions of the cerebral cortex in the adult brain, as previously shown for mouse embryonic cortical neurons (Gaillard et al., 2007).

Another striking aspect of ESC-derived corticogenesis relates to the links between cortical developmental timing and evolution. The protracted periods of human ESC-derived progenitor amplification and neuronal production are highly reminiscent of the extended period of human corticogenesis that allows the generation of a greater number of cortical neurons (Caviness et al., 1995; Lui et al., 2011; Rakic, 2009). ESC-derived intrinsic corticogenesis will thus enable the properties of mouse and human cortical progenitors that underlie their species-specific neurogenic potential to be directly compared (Fietz et al., 2010; Hansen et al., 2010). Similarly, the mechanisms underlying the slow rate of maturation of human ESC cortical neurons, including dendritic and axonal outgrowth and synaptogenesis, could provide hints on the origin of the neoteny that is thought to characterize human cortical synaptogenesis and plasticity (Defelipe, 2011; Petanjek et al., 2011). Comparison of nonhuman and human ESC-derived corticogenesis could also be used to study the growing number of genes displaying human-specific signatures of evolution in the context of brain development (Johnson et al., 2009; Lambert et al., 2011; Pollard et al., 2006; Sudmant et al., 2010).

The combination of human genetics, comparative genomics, and embryology, together with pluripotent stem cell-derived corticogenesis and xenografting, may thus pave the way to the elucidation of the mechanisms underlying the generation of the most complex structure in our brain and some of its most severe pathologies.

EXPERIMENTAL PROCEDURES

ESC/iPSC Differentiation into Cortical Cells

For the differentiation, on day −2, cells were dissociated using Stem-Pro Accutase (Invitrogen A11105) and plated on matrigel (BD, hES qualified matrigel) or on poly-Lysine (BD 354210 33.3 mg/ml)/Laminin (BD 354232 3.3 mg/ml) coated-coverslips/dishes at low confluency (5,000–10,000 cells/cm^2) in MEF-conditioned hES/hiPS medium supplemented with ROCK inhibitor (Y-27632; 10 μM Calbiochem, 688000). When testing cell culture substrates, we found that poly-Lysin/Laminin and Matrigel both resulted in a similar degree of cortical specification, but the latter was used preferentially in the subsequent experiments as it improved cell adhesion considerably. On day 0 of the differentiation, the medium was changed to DDM (Gaspard et al., 2009), supplemented with B27 (10 ml B27 per 500 ml DDM, to increase survival) and Noggin (100 ng/ml), and the medium was replenished every 2 days. After 16 DIV, the medium was changed to DDM, supplemented with B27, and changed every 2 days. At 24 DIV, the progenitors were manually dissociated and cells were resuspended in DDM supplemented with B27 and ROCK inhibitor (10 μM) and plated onto poly-Lysin/Laminin-coated coverslips. Five to seven days after dissociation, half of the medium was replenished with Neurobasal supplemented with B27 (10 ml B27 per 500 ml DDM) and 2 mM glutamine and changed again every 5–7 days. For experiments comparing mouse and human ESC differentiation, cyclopamine was also added at 2–10 DIV.

Intracerebral Grafting

Grafting experiments in newborn mouse motor cortex were performed as previously described (Gaspard et al., 2008), using CD1 (for analysis at 1 month) and NOD/SCID mice (for analysis at 2, 6, and 9 months, as immunosupression was mandatory to achieve integration beyond 2 months). Human ESC-derived progenitors and neurons were manually dissociated at day 24 in culture supplemented with ROCK inhibitor (10 μM). About 100,000–200,000 cells were injected. Analyses on each time point after transplantation were performed on two independent transplantation procedures using three different sets of in vitro differentiations, which yielded similar results. A total number of 34 cases were analyzed (n = 10 for 1 month, 12 for 2 months, 6 for 6 months, and 6 for 9–10 months).

Axonal Tracing

Thalamic input to the graft and grafted neurons projecting to the thalamus were traced with biotin dextran amine (BDA; 10,000 molecular weight; Molecular Probes) and applied iontophoretically into the ipsilateral dorsal lateral geniculate nucleus (DLG).

(B) Sample raw voltage trace of a cell, in response to hyperpolarizing and depolarizing current steps: the firing response is reminiscent of a regular firing accommodating-type cell. The bottom inset shows the first (blue) and the last (green) spike, while the top inset shows the temporal evolution of the instantaneous firing rate.

(C) Single-cell properties: open circles indicate values from single experiments (n = 9), filled circles represent the population mean, and error bars show SEM. Resting membrane potentials V_{rest}, AP firing thresholds V_{th}, input resistances R_m, membrane capacitances C_m, rheobase currents I_{th}, and the slope (gain) of the frequency-current curve represent typical signatures of cortical neurons passive and active electrical properties.

(D) Sample raw voltage traces before (left) and after (right) the bath application of ionotropic glutamatergic receptors antagonists (i.e., CNQX and AP-V).

(E) Spontaneous postsynaptic potential (PSP) properties, extracted by fitting each spontaneous event with a double exponential function: open circles indicate values obtained from distinct ESC-derived neurons (n = 7), filled circles represent the population mean, and error bars show the SEM. The rise time τ_r, decay time τ_d, and the maximal PSP amplitudes represent typical signatures of the activation of proximal AMPA receptor (AMPAR)-mediated glutamatergic synapses. The inset shows a representative single PSP waveform (black) and its fit (red).

(F) Episodic occurrence of increase in background synaptic activity and interictal-like firing: increase in synchronous spontaneous PSPs induces strong voltage fluctuations and a transient membrane depolarization, ultimately leading to the firing of several APs (truncated to allow an expanded view of subthreshold voltage fluctuations). The inset shows a zoom of the area highlighted in yellow.

(G) Sample raw voltage traces, in response to a train of 11 extracellular electrical stimuli at 20 Hz (timed by the red dashes). The top trace quantifies the evoked response under control artificial cerebrospinal fluid. The subsequent application of selective competitive antagonist of AMPAR and NMDAR (i.e., CNQX and AP-V) blocks glutamatergic responses, significantly suppressing evoked PSPs (central trace). The residual responses were $GABA_A$R-mediated, as demonstrated by the successful reversal of the PSP amplitudes, upon injection of a positive holding current (i.e., from −75 mV to −62 mV that is more depolarized than the Chloride reversal potential).

(H) Evoked PSP properties: open circles indicate values from single experiments (n = 4), filled circles represent the population mean, and error bars show SEM. Rise time τ_r, decay time τ_d, the maximal PSP amplitude, and the paired-pulse amplitude ratio represent typical signatures of the activation of short-term facilitating compound glutamatergic and GABAergic microcircuit afferents.

Grafted neurons projecting to the superior colliculus were traced with Alexa Fluor 568-conjugated Dextran (0.5 μl, 1% in distilled water; Molecular Probes) injected into the ipsilateral superior colliculus (SC).

Calcium Imaging

For calcium dye loading, each coverslip was incubated with Oregon Green BAPTA 1-AM. Imaging was carried out using an Axioskop 2 microscope (Zeiss) equipped with a charge-coupled device camera (iXon +, Andor Technology). For pharmacological experiment, TTX (1 μM) was applied by superfusion.

In Vitro Electrophysiology

Whole-cell patch-clamp recordings were performed on individual neurons identified by using infrared differential interference contrast microscopy (Axioskop 2FS, 63×/0.95w, Zeiss). For temporal analysis of functional maturation, 127 cells were recorded from days of differentiation 38 to 82. Cells were classified in two groups as a function of time: early (days 38–65) and late (days 68–82) time points.

Ex Vivo Electrophysiology

Electrophysiology recordings were performed on grafted neurons in acute brain slices from mice at 10 months posttransplantation. Transplanted cells were identified by their enhanced GFP (EGFP) fluorescence and visualized using an upright microscope equipped with infrared differential interference contrast (Leica Microsystems, DMLFS). Some neurons were filled with biocytin during the recordings and were later fixed and stained with streptavidin fluorophore conjugates (see Supplemental Experimental Procedures) for subsequent identification and reconstruction of cell morphology. Whole-cell patch-clamp recordings (EPC 10, HEKA Amplifier Electronics) and bipolar extracellular stimulation (ISO-Flex, AMPI) were performed as described in more detail in the Supplemental Experimental Procedures.

Transcriptome Analyses

Total RNA from two independent samples from ESC-derived cortical differentiations and from fetal cortex samples was extracted using standard procedures (Lambert et al., 2011), and the corresponding cDNAs were prepared and hybridized according to manufacturer's instructions (Affymetrix HGU133+v2.0).

Human Embryonic/Fetal Cortical Samples

The study was approved by the three relevant Ethics Committees (Erasme Hospital, Université Libre de Bruxelles, and Belgian National Fund for Scientific Research FRS/FNRS) on research involving human subjects. Written informed consent was given by the parents in each case.

Additional Methods

An extended version of the experimental procedures is described online in the Supplemental Experimental Procedures.

SUPPLEMENTAL INFORMATION

Supplemental Information includes nine figures, three tables, Supplemental Experimental Procedures, and one movie and can be found with this article online at http://dx.doi.org/10.1016/j.neuron.2012.12.011.

ACKNOWLEDGMENTS

We thank Gilbert Vassart for continuous support and interest, members of the laboratory and IRIBHM for helpful discussions and advice, Viviane De Maertelaer for advice on statistical analyses, Frédéric Bollet-Quivogne (FNRS Logistic Scientist) of the Light Microscopy Facility (LiMiF) for his support with imaging, Marie-Alexandra Lambot for help in the preparation of the human fetal samples, E. Béré for advice on electron microscopy, Delphine Potier and Stein Aerts for their help with microarray data analyses, and Catherine Verfaillie and members of her laboratory for advice on iPSC generation. This work was funded by grants from the Belgian FNRS and FRSM, the Belgian Queen Elizabeth Medical Foundation, the Action de Recherches Concertées (ARC) Programs, the Interuniversity Attraction Poles Program (IUAP) initiated by the Belgian Science Policy Office, the Welbio and Programme d'Excellence CIBLES of the Walloon Region, the Fondations ULB, Pierre Clerdent and Roger de Spoelberch (to P.V.), and the Agence Nationale de la Recherche (grant N°ANR-09-MNPS-027-01, to A.G). M.G. and D.L. are supported by the European Commission (7th Framework Programme, MATERA+ Programme) University of Antwerp (NOI-BOF2009), the Flemish agency for Innovation by Science and Technology (grant 90455/1955, http://www.iwt.be), and the Flanders Research Foundation (grant 12C9112N, http://www.fwo.be). P.V. is Research Director, I.E-C. is Postdoctoral Fellow, and is N.L. clinical scientist of the FNRS.

Accepted: December 3, 2012
Published: February 6, 2013

REFERENCES

Alcamo, E.A., Chirivella, L., Dautzenberg, M., Dobreva, G., Fariñas, I., Grosschedl, R., and McConnell, S.K. (2008). Satb2 regulates callosal projection neuron identity in the developing cerebral cortex. Neuron *57*, 364–377.

Barnes, A.P., and Polleux, F. (2009). Establishment of axon-dendrite polarity in developing neurons. Annu. Rev. Neurosci. *32*, 347–381.

Bedogni, F., Hodge, R.D., Elsen, G.E., Nelson, B.R., Daza, R.A., Beyer, R.P., Bammler, T.K., Rubenstein, J.L., and Hevner, R.F. (2010). Tbr1 regulates regional and laminar identity of postmitotic neurons in developing neocortex. Proc. Natl. Acad. Sci. USA *107*, 13129–13134.

Bystron, I., Rakic, P., Molnár, Z., and Blakemore, C. (2006). The first neurons of the human cerebral cortex. Nat. Neurosci. *9*, 880–886.

Bystron, I., Blakemore, C., and Rakic, P. (2008). Development of the human cerebral cortex: Boulder Committee revisited. Nat. Rev. Neurosci. *9*, 110–122.

Caviness, V.S., Jr., Takahashi, T., and Nowakowski, R.S. (1995). Numbers, time and neocortical neuronogenesis: a general developmental and evolutionary model. Trends Neurosci. *18*, 379–383.

Chambers, S.M., Fasano, C.A., Papapetrou, E.P., Tomishima, M., Sadelain, M., and Studer, L. (2009). Highly efficient neural conversion of human ES and iPS cells by dual inhibition of SMAD signaling. Nat. Biotechnol. *27*, 275–280.

Defelipe, J. (2011). The evolution of the brain, the human nature of cortical circuits, and intellectual creativity. Front Neuroanat *5*, 29.

Dolmetsch, R., and Geschwind, D.H. (2011). The human brain in a dish: the promise of iPSC-derived neurons. Cell *145*, 831–834.

Eiraku, M., Watanabe, K., Matsuo-Takasaki, M., Kawada, M., Yonemura, S., Matsumura, M., Wataya, T., Nishiyama, A., Muguruma, K., and Sasai, Y. (2008). Self-organized formation of polarized cortical tissues from ESCs and its active manipulation by extrinsic signals. Cell Stem Cell *3*, 519–532.

Fietz, S.A., Kelava, I., Vogt, J., Wilsch-Bräuninger, M., Stenzel, D., Fish, J.L., Corbeil, D., Riehn, A., Distler, W., Nitsch, R., and Huttner, W.B. (2010). OSVZ progenitors of human and ferret neocortex are epithelial-like and expand by integrin signaling. Nat. Neurosci. *13*, 690–699.

Fish, J.L., Dehay, C., Kennedy, H., and Huttner, W.B. (2008). Making bigger brains-the evolution of neural-progenitor-cell division. J. Cell Sci. *121*, 2783–2793.

Gaillard, A., Gaillard, F., and Roger, M. (1998). Neocortical grafting to newborn and adult rats: developmental, anatomical and functional aspects. Adv. Anat. Embryol. Cell Biol. *148*, 1–86.

Gaillard, A., Prestoz, L., Dumartin, B., Cantereau, A., Morel, F., Roger, M., and Jaber, M. (2007). Reestablishment of damaged adult motor pathways by grafted embryonic cortical neurons. Nat. Neurosci. *10*, 1294–1299.

Gaspard, N., and Vanderhaeghen, P. (2011). Laminar fate specification in the cerebral cortex. F1000 Biol. Rep. *3*, 6.

Gaspard, N., Bouschet, T., Hourez, R., Dimidschstein, J., Naeije, G., van den Ameele, J., Espuny-Camacho, I., Herpoel, A., Passante, L., Schiffmann, S.N., et al. (2008). An intrinsic mechanism of corticogenesis from embryonic stem cells. Nature *455*, 351–357.

Gaspard, N., Bouschet, T., Herpoel, A., Naeije, G., van den Ameele, J., and Vanderhaeghen, P. (2009). Generation of cortical neurons from mouse embryonic stem cells. Nat. Protoc. *4*, 1454–1463.

Han, S.S., Williams, L.A., and Eggan, K.C. (2011). Constructing and deconstructing stem cell models of neurological disease. Neuron *70*, 626–644.

Hand, R., Bortone, D., Mattar, P., Nguyen, L., Heng, J.I., Guerrier, S., Boutt, E., Peters, E., Barnes, A.P., Parras, C., et al. (2005). Phosphorylation of Neurogenin2 specifies the migration properties and the dendritic morphology of pyramidal neurons in the neocortex. Neuron *48*, 45–62.

Hansen, D.V., Lui, J.H., Parker, P.R., and Kriegstein, A.R. (2010). Neurogenic radial glia in the outer subventricular zone of human neocortex. Nature *464*, 554–561.

Hansen, D.V., Rubenstein, J.L., and Kriegstein, A.R. (2011). Deriving excitatory neurons of the neocortex from pluripotent stem cells. Neuron *70*, 645–660.

Hébert, J.M., and Fishell, G. (2008). The genetics of early telencephalon patterning: some assembly required. Nat. Rev. Neurosci. *9*, 678–685.

Hevner, R.F. (2006). From radial glia to pyramidal-projection neuron: transcription factor cascades in cerebral cortex development. Mol. Neurobiol. *33*, 33–50.

Hill, R.S., and Walsh, C.A. (2005). Molecular insights into human brain evolution. Nature *437*, 64–67.

Ideguchi, M., Palmer, T.D., Recht, L.D., and Weimann, J.M. (2010). Murine embryonic stem cell-derived pyramidal neurons integrate into the cerebral cortex and appropriately project axons to subcortical targets. J. Neurosci. *30*, 894–904.

Inoue, T., Nakamura, S., and Osumi, N. (2000). Fate mapping of the mouse prosencephalic neural plate. Dev. Biol. *219*, 373–383.

Johnson, M.B., Kawasawa, Y.I., Mason, C.E., Krsnik, Z., Coppola, G., Bogdanović, D., Geschwind, D.H., Mane, S.M., State, M.W., and Sestan, N. (2009). Functional and evolutionary insights into human brain development through global transcriptome analysis. Neuron *62*, 494–509.

Lambert, N., Lambot, M.A., Bilheu, A., Albert, V., Englert, Y., Libert, F., Noel, J.C., Sotiriou, C., Holloway, A.K., Pollard, K.S., et al. (2011). Genes expressed in specific areas of the human fetal cerebral cortex display distinct patterns of evolution. PLoS ONE *6*, e17753.

Leone, D.P., Srinivasan, K., Chen, B., Alcamo, E., and McConnell, S.K. (2008). The determination of projection neuron identity in the developing cerebral cortex. Curr. Opin. Neurobiol. *18*, 28–35.

Li, X.J., Zhang, X., Johnson, M.A., Wang, Z.B., Lavaute, T., and Zhang, S.C. (2009). Coordination of sonic hedgehog and Wnt signaling determines ventral and dorsal telencephalic neuron types from human embryonic stem cells. Development *136*, 4055–4063.

Lui, J.H., Hansen, D.V., and Kriegstein, A.R. (2011). Development and evolution of the human neocortex. Cell *146*, 18–36.

Marchetto, M.C., Winner, B., and Gage, F.H. (2010). Pluripotent stem cells in neurodegenerative and neurodevelopmental diseases. Hum. Mol. Genet. *19*(R1), R71–R76.

McCormick, D.A., Connors, B.W., Lighthall, J.W., and Prince, D.A. (1985). Comparative electrophysiology of pyramidal and sparsely spiny stellate neurons of the neocortex. J. Neurophysiol. *54*, 782–806.

McKenna, W.L., Betancourt, J., Larkin, K.A., Abrams, B., Guo, C., Rubenstein, J.L., and Chen, B. (2011). Tbr1 and Fezf2 regulate alternate corticofugal neuronal identities during neocortical development. J. Neurosci. *31*, 549–564.

Molnár, Z., and Cheung, A.F. (2006). Towards the classification of subpopulations of layer V pyramidal projection neurons. Neurosci. Res. *55*, 105–115.

Molyneaux, B.J., Arlotta, P., Menezes, J.R., and Macklis, J.D. (2007). Neuronal subtype specification in the cerebral cortex. Nat. Rev. Neurosci. *8*, 427–437.

O'Leary, D.D., and Sahara, S. (2008). Genetic regulation of arealization of the neocortex. Curr. Opin. Neurobiol. *18*, 90–100.

Okano, H., and Temple, S. (2009). Cell types to order: temporal specification of CNS stem cells. Curr. Opin. Neurobiol. *19*, 112–119.

Paxinos, G.F., and Franklin, K.B.J. (1997). The Mouse Brain in Stereotaxic Coordinates (San Diego, CA: Academic Press).

Pera, M.F., Andrade, J., Houssami, S., Reubinoff, B., Trounson, A., Stanley, E.G., Ward-van Oostwaard, D., and Mummery, C. (2004). Regulation of human embryonic stem cell differentiation by BMP-2 and its antagonist noggin. J. Cell Sci. *117*, 1269–1280.

Petanjek, Z., Judaš, M., Šimic, G., Rasin, M.R., Uylings, H.B., Rakic, P., and Kostovic, I. (2011). Extraordinary neoteny of synaptic spines in the human prefrontal cortex. Proc. Natl. Acad. Sci. USA *108*, 13281–13286.

Pinaudeau, C., Gaillard, A., and Roger, M. (2000). Stage of specification of the spinal cord and tectal projections from cortical grafts. Eur. J. Neurosci. *12*, 2486–2496.

Pollard, K.S., Salama, S.R., Lambert, N., Lambot, M.A., Coppens, S., Pedersen, J.S., Katzman, S., King, B., Onodera, C., Siepel, A., et al. (2006). An RNA gene expressed during cortical development evolved rapidly in humans. Nature *443*, 167–172.

Rakic, P. (1995). A small step for the cell, a giant leap for mankind: a hypothesis of neocortical expansion during evolution. Trends Neurosci. *18*, 383–388.

Rakic, P. (2009). Evolution of the neocortex: a perspective from developmental biology. Nat. Rev. Neurosci. *10*, 724–735.

Reyes, A., and Sakmann, B. (1999). Developmental switch in the short-term modification of unitary EPSPs evoked in layer 2/3 and layer 5 pyramidal neurons of rat neocortex. J. Neurosci. *19*, 3827–3835.

Shi, Y., Kirwan, P., Smith, J., Robinson, H.P., and Livesey, F.J. (2012). Human cerebral cortex development from pluripotent stem cells to functional excitatory synapses. Nat. Neurosci. *15*, 477–486, S1.

Sudmant, P.H., Kitzman, J.O., Antonacci, F., Alkan, C., Malig, M., Tsalenko, A., Sampas, N., Bruhn, L., Shendure, J., and Eichler, E.E.; 1000 Genomes Project. (2010). Diversity of human copy number variation and multicopy genes. Science *330*, 641–646.

Sur, M., and Rubenstein, J.L. (2005). Patterning and plasticity of the cerebral cortex. Science *310*, 805–810.

Vanderhaeghen, P., and Polleux, F. (2004). Developmental mechanisms patterning thalamocortical projections: intrinsic, extrinsic and in between. Trends Neurosci. *27*, 384–391.

Walther, C., and Gruss, P. (1991). Pax-6, a murine paired box gene, is expressed in the developing CNS. Development *113*, 1435–1449.

Wang, Y., Markram, H., Goodman, P.H., Berger, T.K., Ma, J., and Goldman-Rakic, P.S. (2006). Heterogeneity in the pyramidal network of the medial prefrontal cortex. Nat. Neurosci. *9*, 534–542.

Wilson, S.W., and Houart, C. (2004). Early steps in the development of the forebrain. Dev. Cell *6*, 167–181.

Zeng, H., Guo, M., Martins-Taylor, K., Wang, X., Zhang, Z., Park, J.W., Zhan, S., Kronenberg, M.S., Lichtler, A., Liu, H.X., et al. (2010). Specification of region-specific neurons including forebrain glutamatergic neurons from human induced pluripotent stem cells. PLoS ONE *5*, e11853.

Zhang, X., Huang, C.T., Chen, J., Pankratz, M.T., Xi, J., Li, J., Yang, Y., Lavaute, T.M., Li, X.J., Ayala, M., et al. (2010). Pax6 is a human neuroectoderm cell fate determinant. Cell Stem Cell *7*, 90–100.